

Electronic Supporting Information

Lead-free Perovskite $[\text{H}_3\text{NC}_6\text{H}_4\text{NH}_3]\text{CuBr}_4$ with both a Band-Gap of 1.43 eV and Excellent Stability

Xiaolei Li, Zhen Li, Gao Zhang, and Guan-Jun Yang*

School of Materials Science and Engineering, Xi'an Jiaotong University, Xi'an 710049, P. R.
China

Corresponding author:

*Guanjun Yang, E-mail: ygj@mail.xjtu.edu.cn.

Experimental Section

Materials:

All the chemicals were used as received, including CuBr₂ (Copper bromide, 99.999%, Sigma-Aldrich), BrH₃NC₆H₄NH₃Br (1,4-Benzenediammonium bromide, 98%, Xi'an Polymer Light Technology Corp), dimethylformamide (DMF, anhydrous, 99.8%, Sigma-Aldrich), and dimethylsulfoxide (DMSO, anhydrous, 99.8%, Sigma-Aldrich). Fluorine-doped tin oxide (FTO)-coated glass (TEC7, 2.2 mm) and indium tin oxide (ITO)/PET (0.125 ± 0.05 mm) were purchased from Ying Kou You Xuan Trade Co., Ltd (China).

Film fabrication:

The pPDACuBr₄ precursor solution (0.5 mol/L) was formed by dissolving equimolar BrH₃NC₆H₄NH₃Br (269.9 mg) and CuBr₂ (223.5 mg) in mixed solvents including 0.6 mL of DMF and 1.4 mL of DMSO. Then, the precursor solution was stirred at 60°C overnight. For the hot-casting method,¹ the pPDACuBr₄ precursor solution and FTO glasses were heated on a hot plate at 70°C and 120°C respectively for 10 min. Then the pPDACuBr₄ precursor solution (Figure 1c) was dropped on the pre-heated FTO substrates and spin-coated at 3000 rpm for 20 s. For conventional post-annealing method, the pPDACuBr₄ precursor solution was dropped on FTO substrates and spin-coated at 3000 rpm for 20 s. All perovskite films were annealed at 90°C for 20 min.

Material characterizations:

Powder X-ray diffraction (XRD) measurements were performed on a Ultima IV X-ray Diffractometer with Cu K α from 5 to 80° (2 θ). UV-vis and transmission spectra were measured for the pPDACuBr₄ thin films spin-coated on the FTO substrate using a PerkinElmer Lambda 950 spectrophotometer. SEM tests were performed on a field-emission SEM (MIRA3 TESCAN). Transient steady-state fluorescence spectrometer (Edinburgh FLS9) was used to test the steady-state photoluminescence (PL) spectrum (Excitation wavelength: 635 nm). An SDT Q600 V20.5 Build 15 instrument was used for thermogravimetric analysis. The analysis was performed under a nitrogen atmosphere (flow rate 60 mL/min), and an interval from 42 to 800°C (ramp rate of 10°C/min) was studied. The film thickness for calculation of absorption coefficient (see Figure S6) was measured by a Profilometer Dektak XT (Brucker). The samples for UV-vis and transmission spectroscopy tests were prepared by the hot-casting method. The UV light stability tests were carried using a 250 W (wavelength: 395 nm) UV lamp.

Solar cell fabrication and characterizations:

The FTO glasses were cleaned sequentially in acetone, ethanol, and deionized water, each for 15 min respectively, and then dried by Nitrogen and treated in UV Ozone for 30 min. A SnO₂ nanoparticle-modified TiO₂ film (SnO₂@TiO₂) was prepared according to our previously report. The FTO substrates coated with SnO₂@TiO₂ layer were preheated at 120°C for 10 min. Then 0.5 M pPDACuBr₄ precursor in DMF and DMSO (Volume ratio 3:7) solution was dropped on the substrates and spin coated at 3000 rpm for 20 s. Then, the perovskite films were heated at 120°C for 10 min. The hole transport layer (HTL) was prepared by spin-coating the Spiro-OMeTAD solution at 3000 rpm for 30 s. Finally, 100 nm of Au metal electrode was thermally evaporated onto the HTL. Photocurrent-voltage (*J-V*) curves of the devices with an active area of 0.1 cm² were tested by using a source meter (2400, Keithley) under AM 1.5 G condition of 100 mW/cm² illumination using a Peccell Technologies PEC-L01 solar simulator. The devices were tested by forward (from -0.2 to 1.2 V) voltage scanning with a sweep speed of 0.05 V/s.

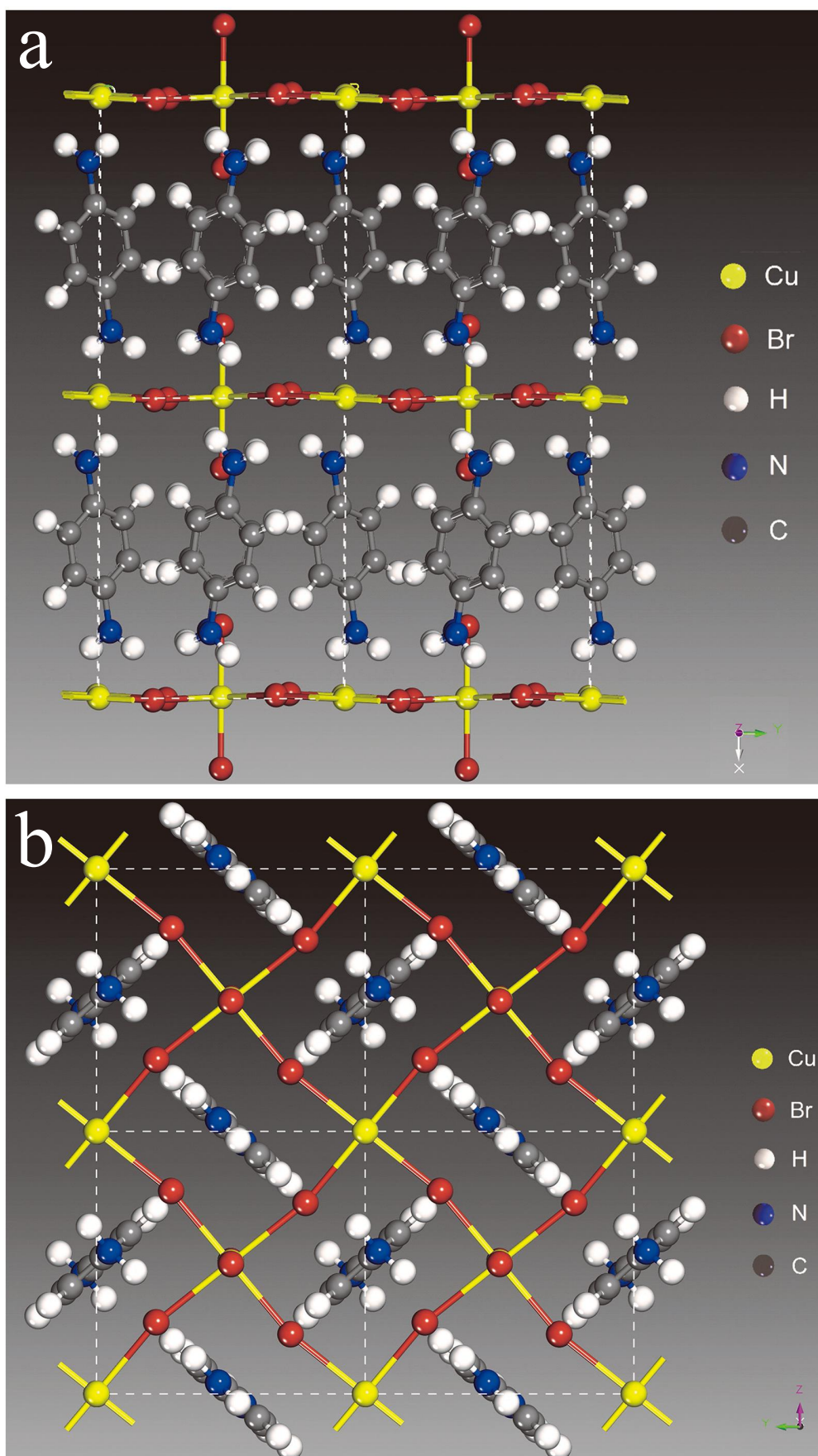


Figure S1. Different perspectives of the pPDACuBr₄ structure from (a) top view and (b) side view.

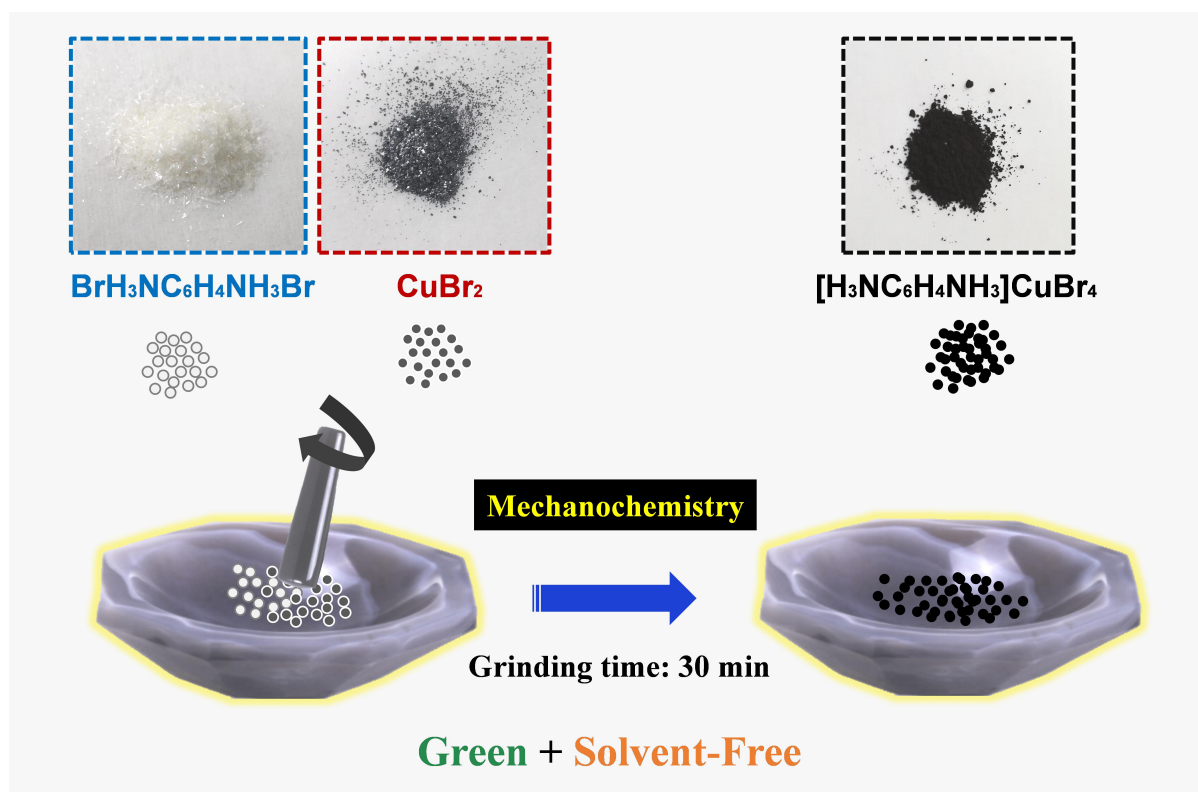


Figure S2. Illustration of the synthesis of pPDACuBr₄ powders via a mechanochemistry method. The pPDACuBr₄ powders were fabricated by grinding the mixture of equimolar BrH₃NC₆H₄NH₃Br and CuBr₂ powders in a mortar for 30 min. Then the compound powders were heated at 50°C for 30 min to promote the chemical reaction. Finally, to prevent the residue of the reactant remaining in the mixture, the powders were ground for another 10 min, after we got the black pPDACuBr₄ powders.

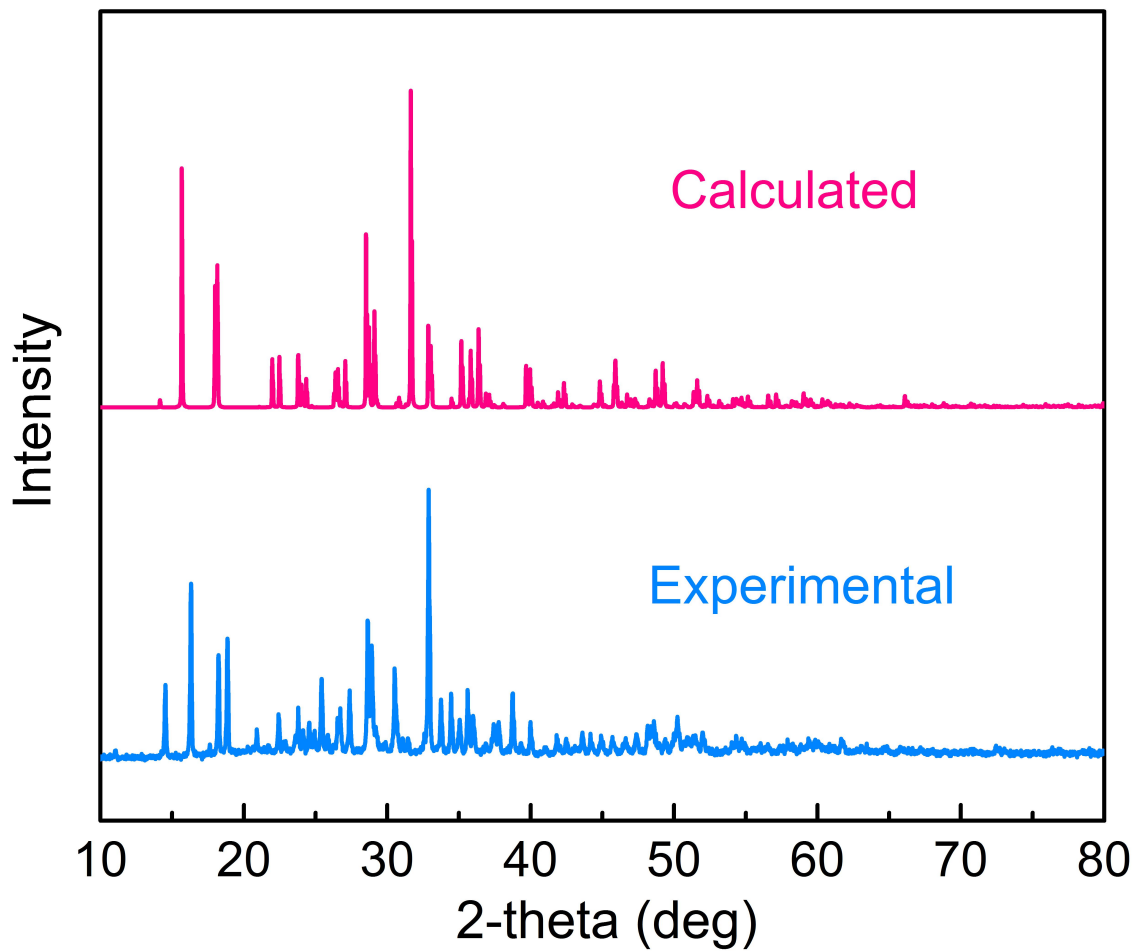


Figure S3. XRD patterns of experimental and calculated pPDACuBr₄ perovskites. The calculated XRD pattern was performed using Reflex module package in Materials Studio.^{3,4}

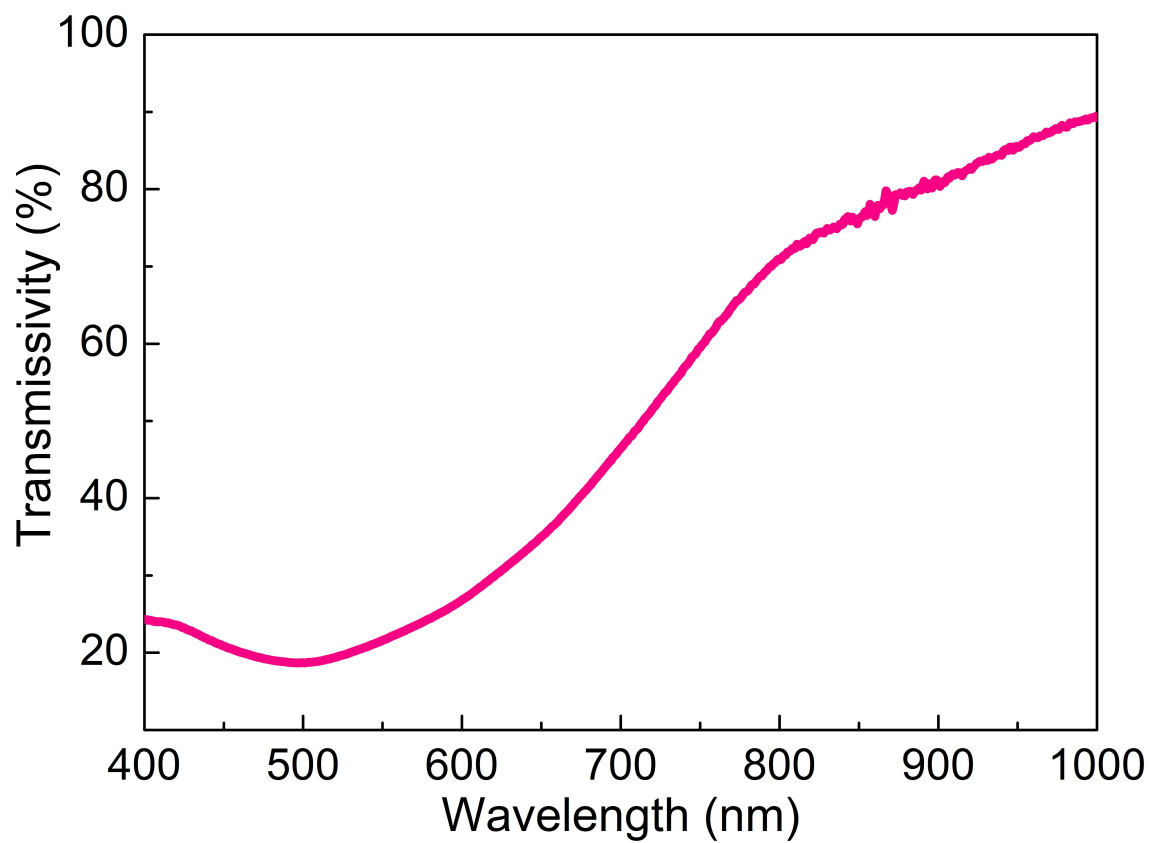


Figure S4. Transmittance spectrum of a pPDACuBr₄ film spin-coated on FTO glass.

Table S1. Bandgaps of various halide perovskite materials reported in the literature.

Types	Compound	Bandgap (eV)	Ref.
Pb-based	MAPbI ₃	1.55	[5]
	FAPbI ₃	1.50	[5]
	CsPbI ₃	1.67	[6]
Sn-based	FASnI ₃	1.41	[6]
	MASnI ₃	1.20	[6]
	CsSnI ₃	1.30	[6]
Ge-based	MAGeI ₃	1.90	[7]
	FAGeI ₃	2.20	[7]
	CsGeI ₃	1.60	[7]
Bi-based	Cs ₂ Ag(Bi _{0.625} Sb _{0.375})Br ₆	1.86	[8]
	AgBi ₂ I ₇	1.87	[9]
	Rb ₃ Bi ₂ I ₉	2.10	[6]
	C ₆ H ₅ NH ₃ BiI ₄	2.14	[10]
Sb-based	MA ₃ Sb ₂ I ₉	2.14	[11]
	Cs ₂ SbAgCl ₆ (Cu ²⁺ -doped)	1.00	[12]
	Cs ₄ CuSb ₂ Cl ₁₂	1.00	[13]
Ti-based	Cs ₂ TiI ₂ Br ₄	1.38	[14]
Cu-based	(C ₆ H ₅ CH ₂ NH ₃) ₂ CuBr ₄	1.80	[15]
	MA ₂ CuCl _{0.5} Br _{3.5}	1.80	[16]
	pPDACuBr ₄	1.43	Our work

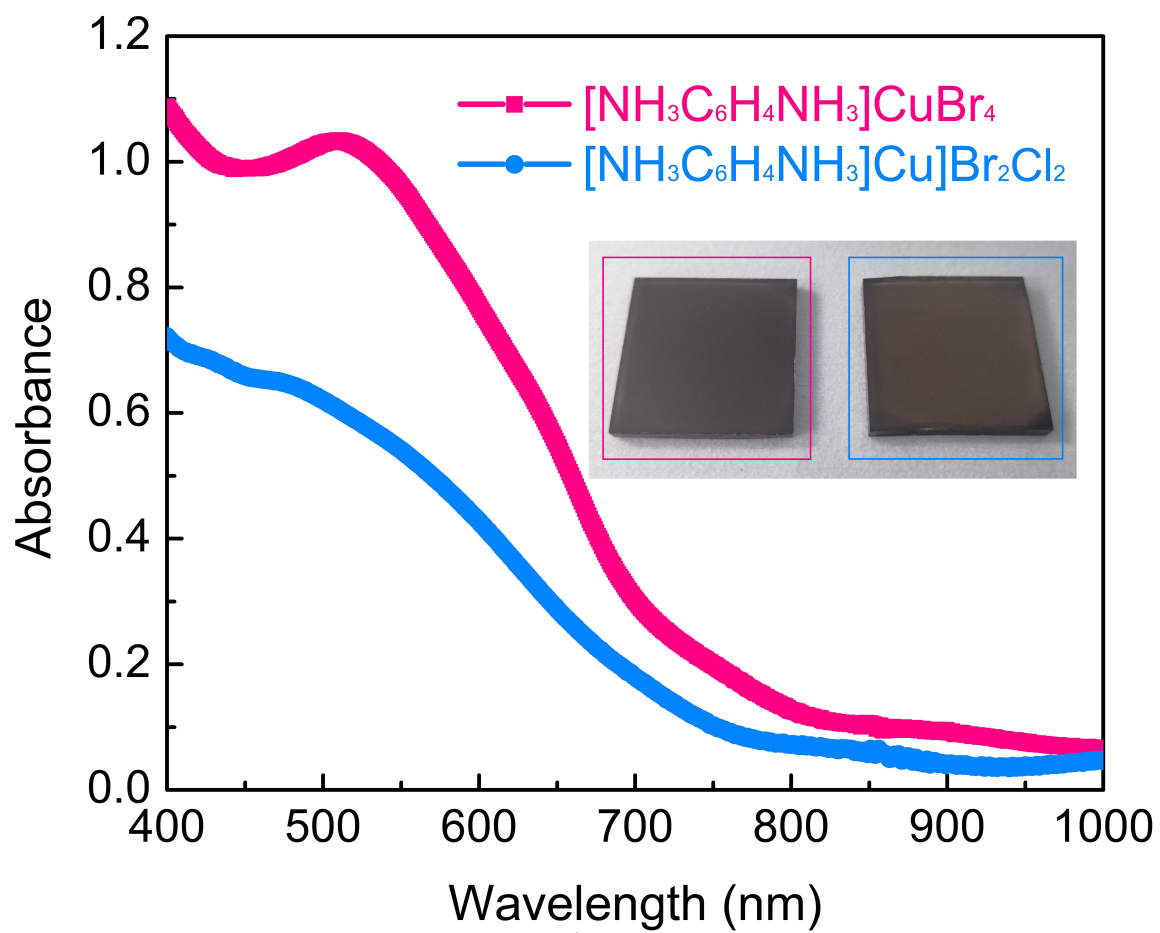


Figure S5. UV-vis absorption spectra of pPDACuBr₄ and pPDACuBr₂Cl₂ films. Inset: digital photographs of pPDACuBr₄ (left) and pPDACuBr₂Cl₂ (right) films.

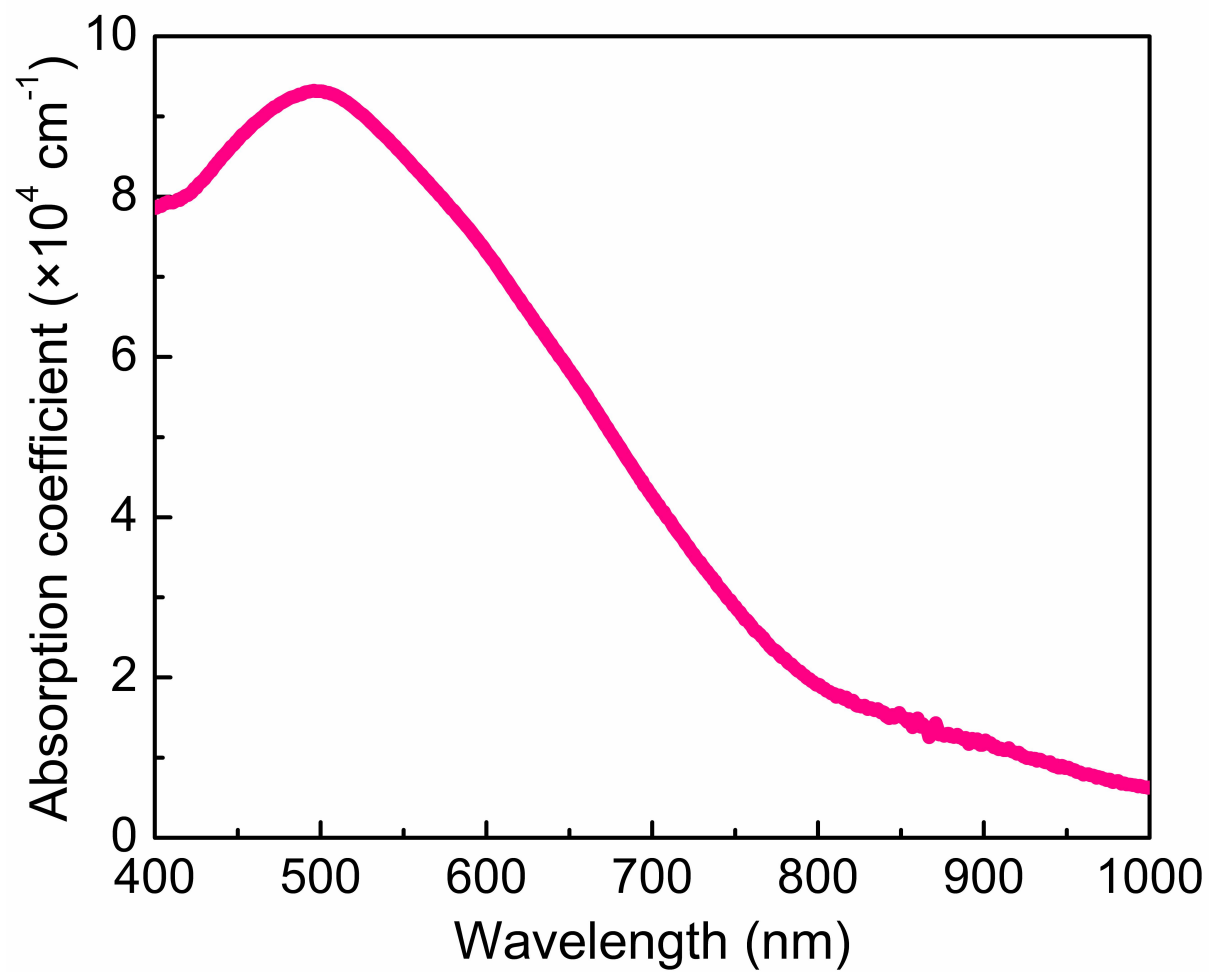


Figure S6. Absorption coefficient of a pPDACuBr₄ film at a wavelength from 400 nm to 1000 nm (The film thickness is about 180 nm).

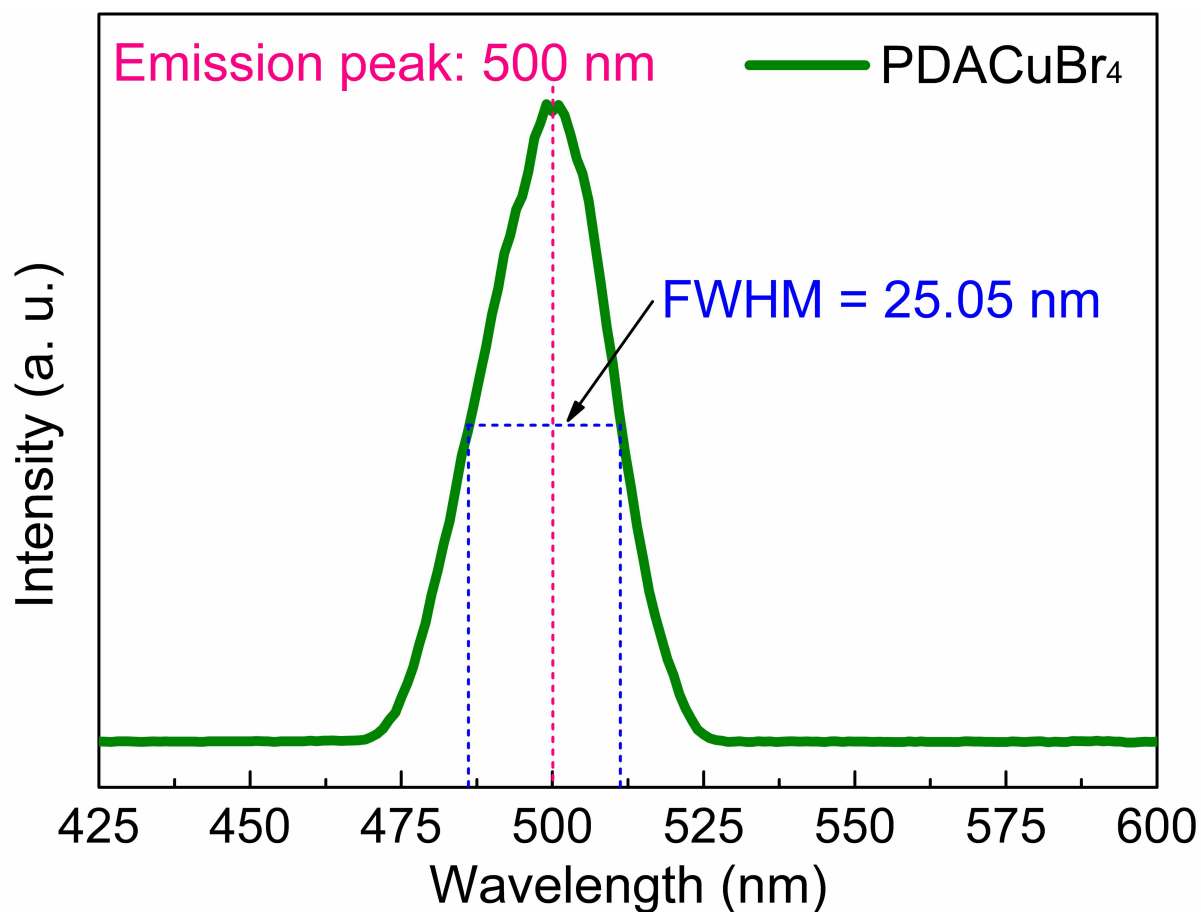


Figure S7. Steady-state photoluminescence spectrum of a pPDACuBr₄ film.

Table S2. Optical parameter comparison of Cu-based perovskite materials.

Perovskites	Emission peak [nm]	FWHM [nm]	Spectral region	Ref.
MA ₂ CuCl ₂ Br ₂ powders	~513	~83	green	[16]
MA ₂ CuCl _{0.5} Br _{3.5} powders	~520	~75	green	[16]
Cs ₂ CuCl ₄ QDs	388	68	blue-green	[17]
Cs ₂ CuBr ₄ QDs	393	74	blue-green	[17]
pPDACuBr ₄ film	500	25.05	green	Our work

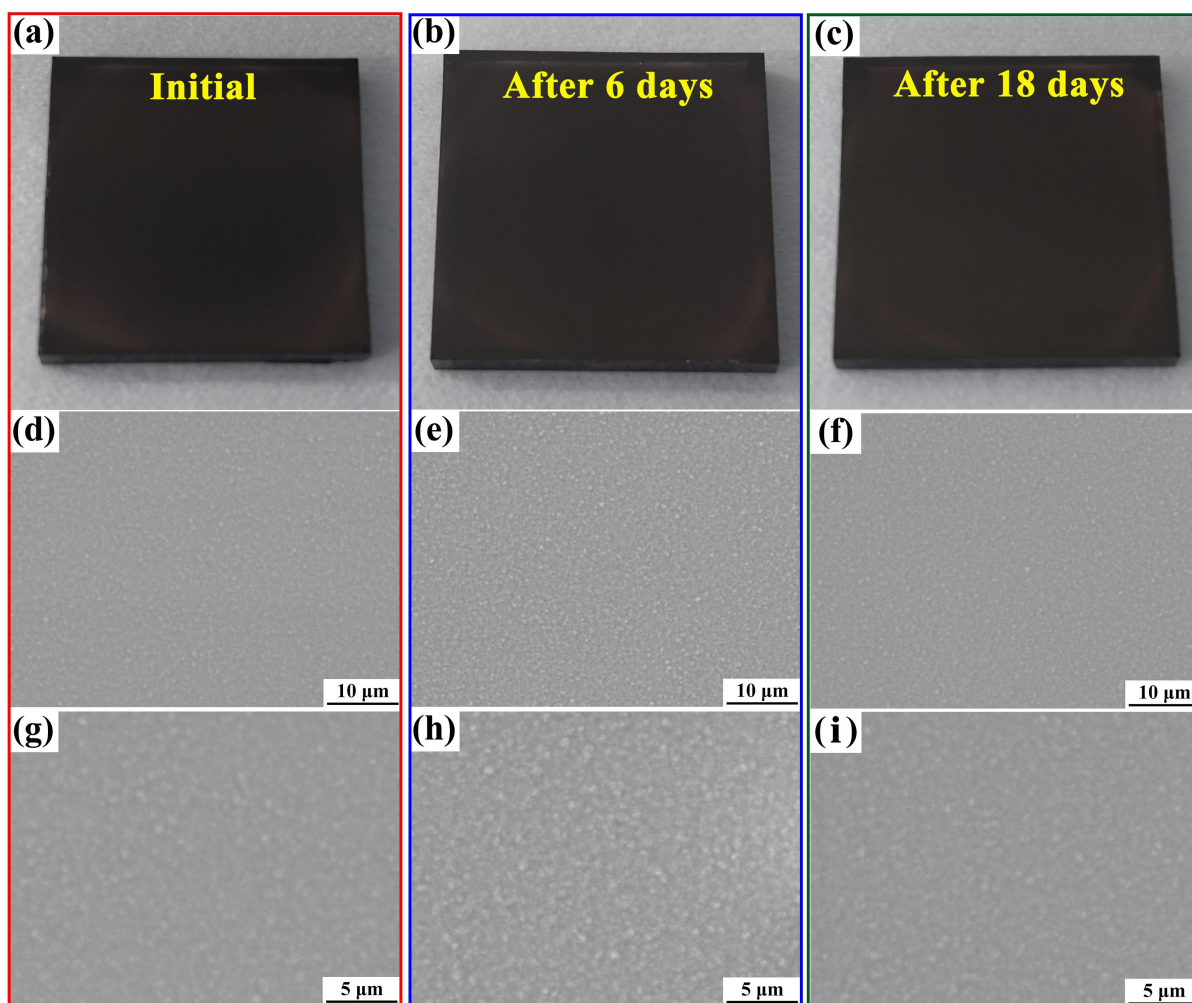


Figure S8. Photographs and SEM images of a pPDACuBr₄ film before (a, d, g) and after storage in ambient air (relative humidity: 40-50%, temperature: ~25 °C) for 6 (b, e, h) and 18 (c, f, i) days.

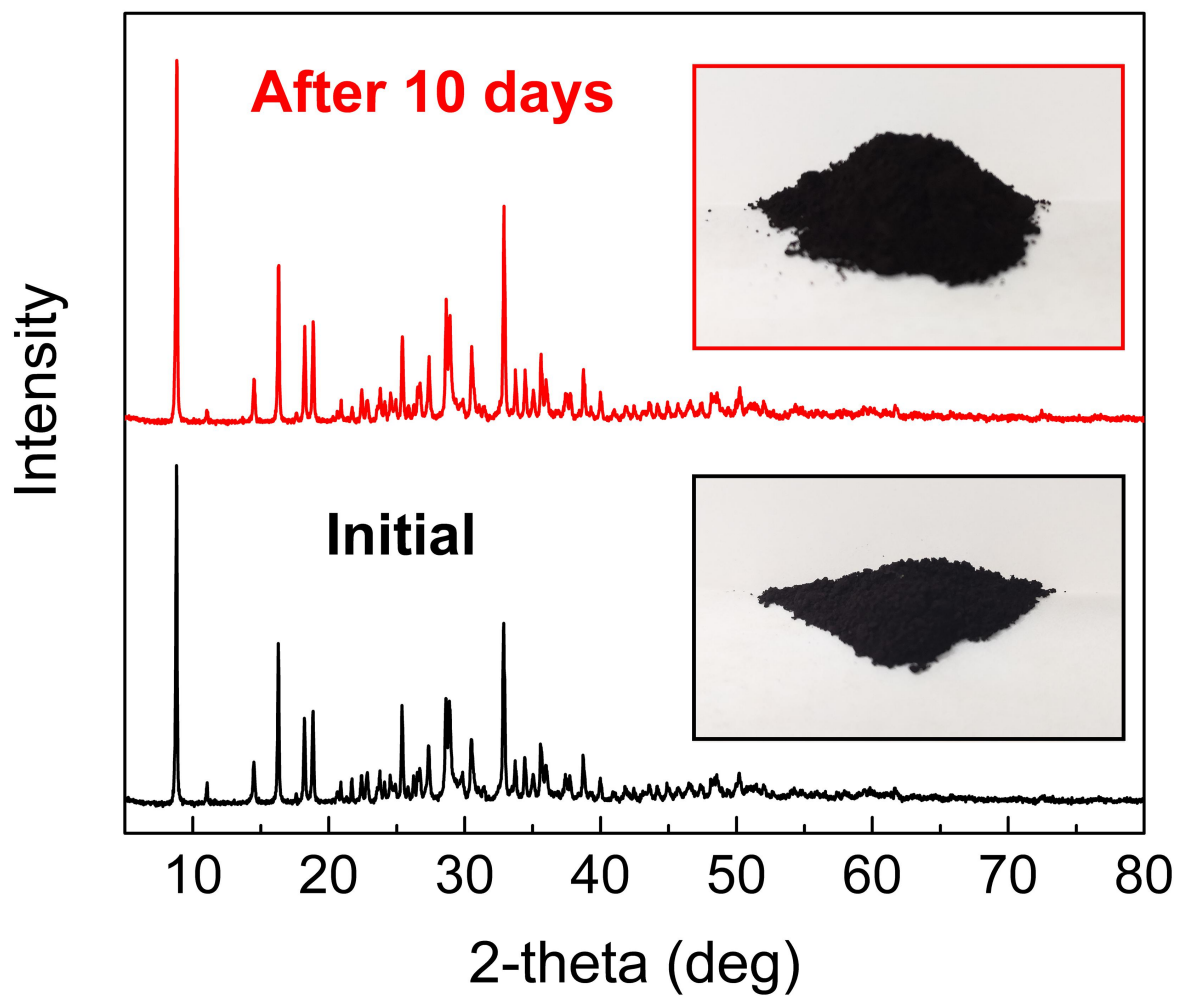


Figure S9. XRD patterns and photographs of pPDACuBr₄ materials before and after storage in ambient air (relative humidity: 40-50%, temperature: ~25 °C) for 10 days.

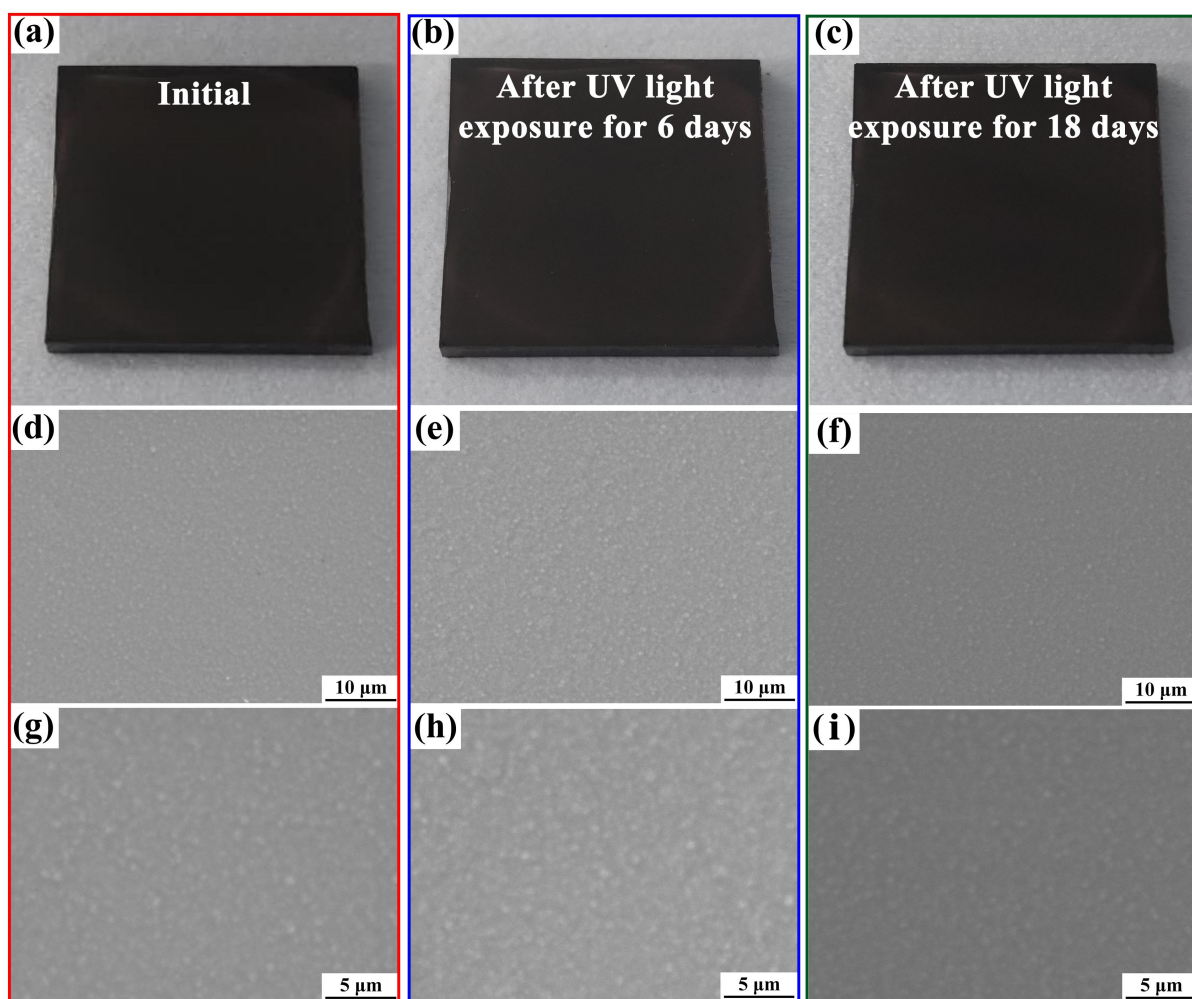


Figure S10. Photographs and SEM images of a pPDACuBr₄ film before (a, d, g) and after continuous UV light exposure for 6 (b, e, h) and 18 (c, f, i) days.

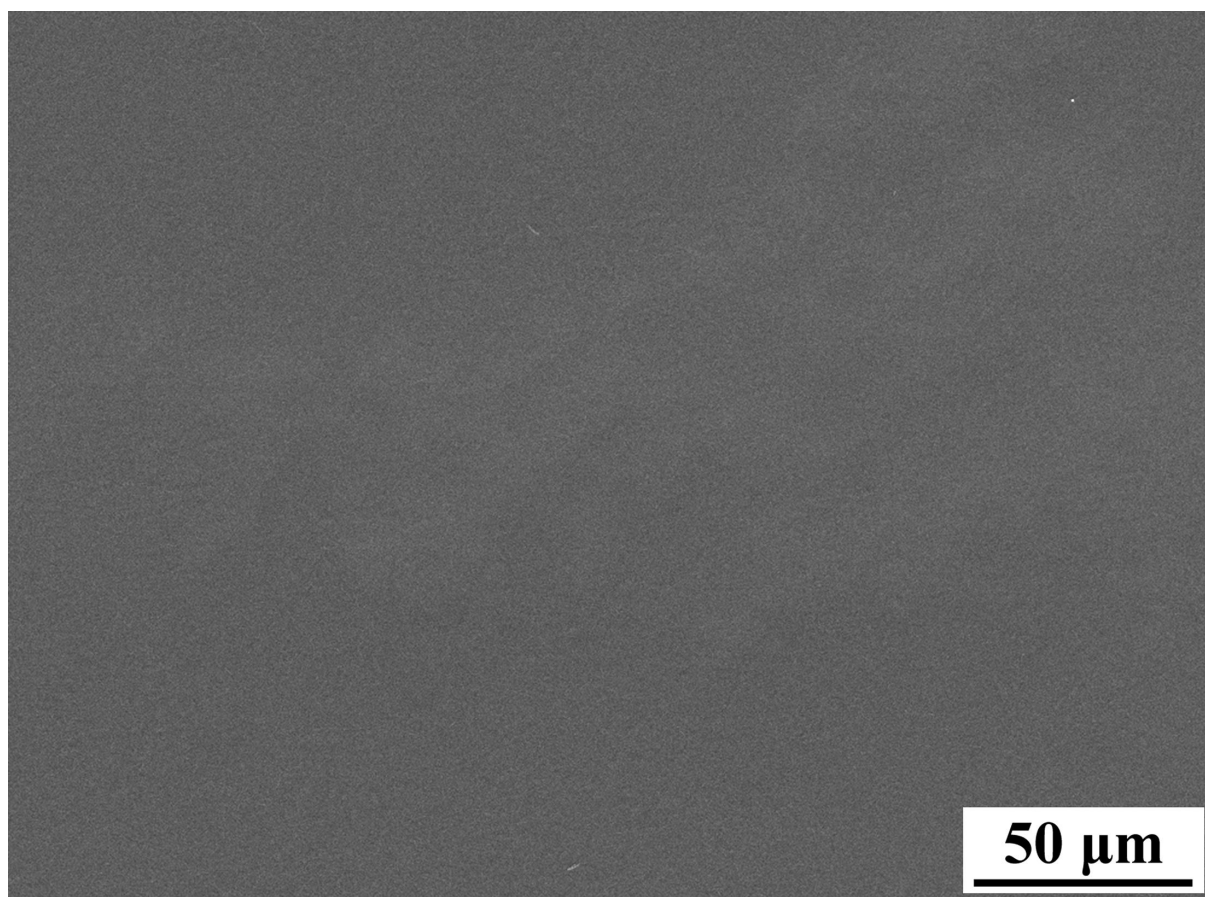


Figure S11. SEM image of a pPDACuBr₄ film prepared by hot-casting method at low magnification (1000x).

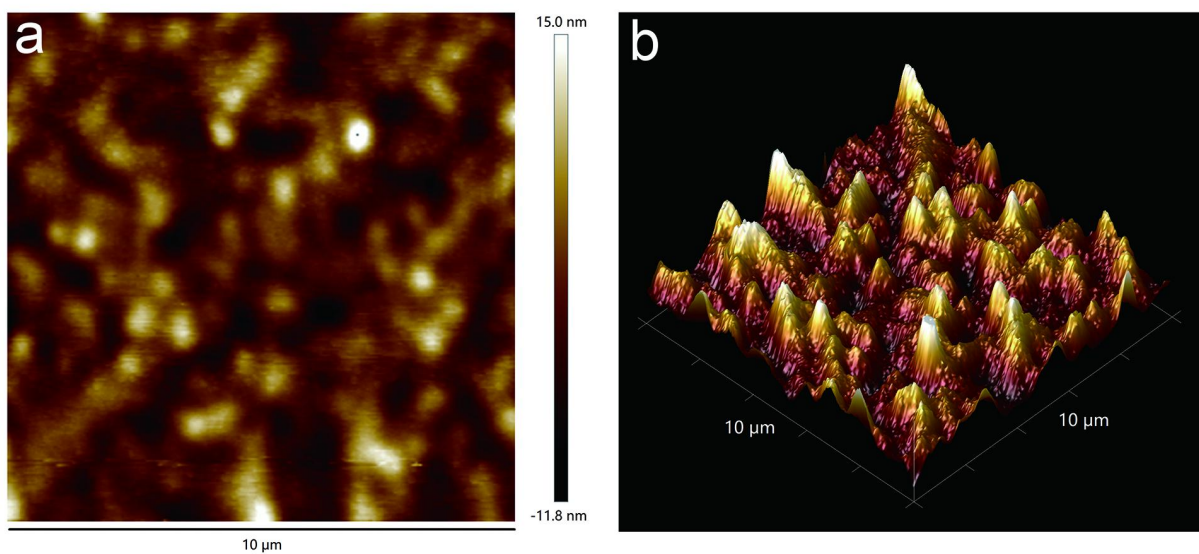


Figure S12. AFM height image (a) and 3D image (b) of pPDACuBr₄ film prepared by hot-casting method.

Table S3. Roughness comparison between respective MAPbI₃ films prepared by different methods and the pPDACuBr₄ film prepared by hot-casting method.

Perovskites	Root mean square roughness (nm)	Scanning area (μm ²)	Methods	Ref.
MAPbI ₃	7.90	10 × 10	Gas pump	[18]
	4.98	5 × 5	Multi-flow air knife	[19]
	8.30	3 × 3	Solvent engineering	[20]
	14.5	—	Surfactant-controlled ink	[21]
pPDACuBr ₄	3.85	10 × 10	Hot-casting	Our work

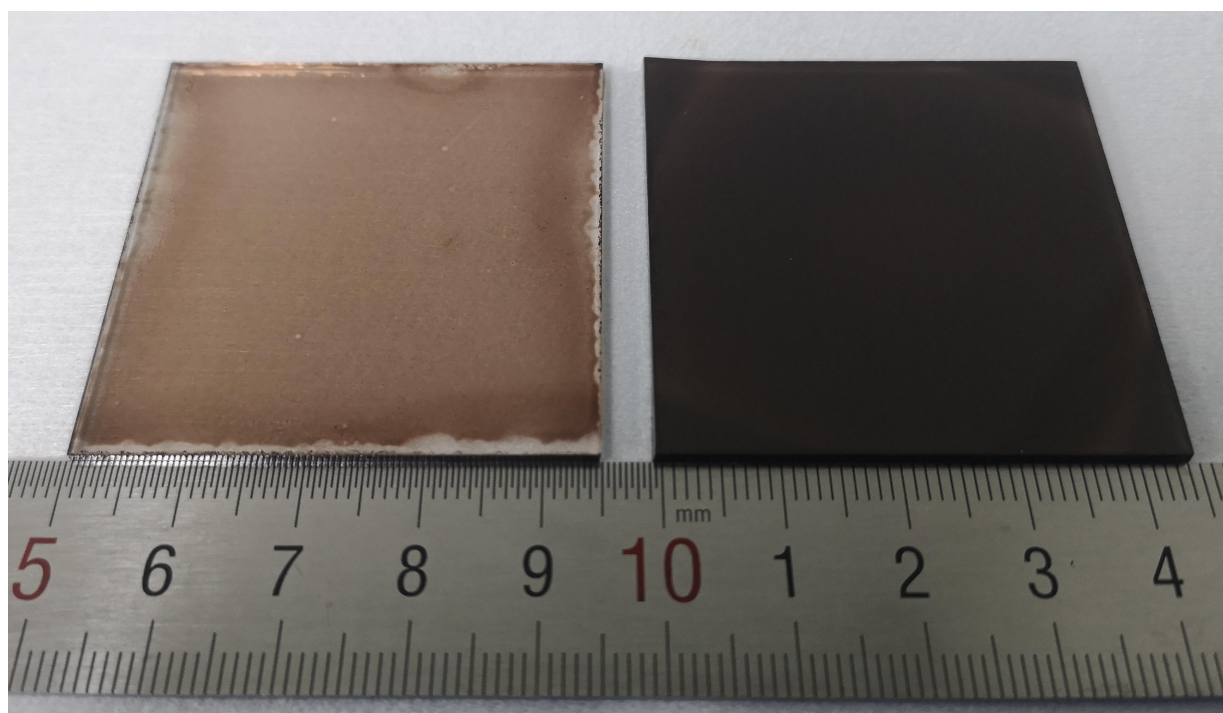


Figure S13. Digital photographs of pPDACuBr₄ films prepared by conventional post-annealing (left) and hot-casting (right).

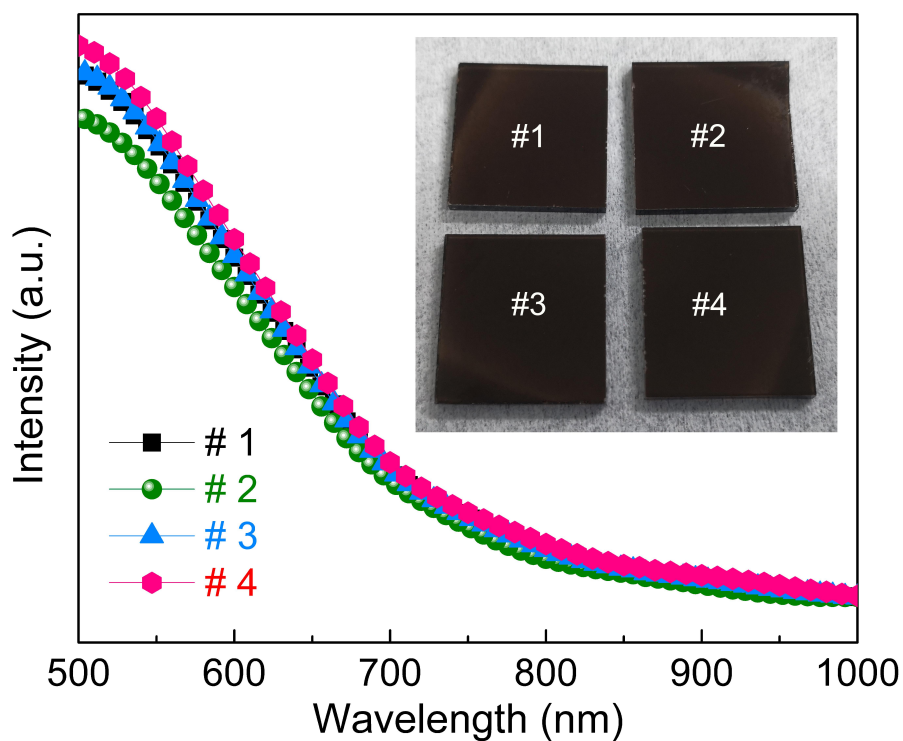


Figure S14. The UV-vis light absorption spectra of 4 pieces of 2.25 cm \times 2.25 cm perovskite films. The films were made by cutting an 4.5 cm \times 4.5 cm film into 4 pieces: the spectra of each piece was recorded individually. The perovskite film was deposited via the hot-casting method.

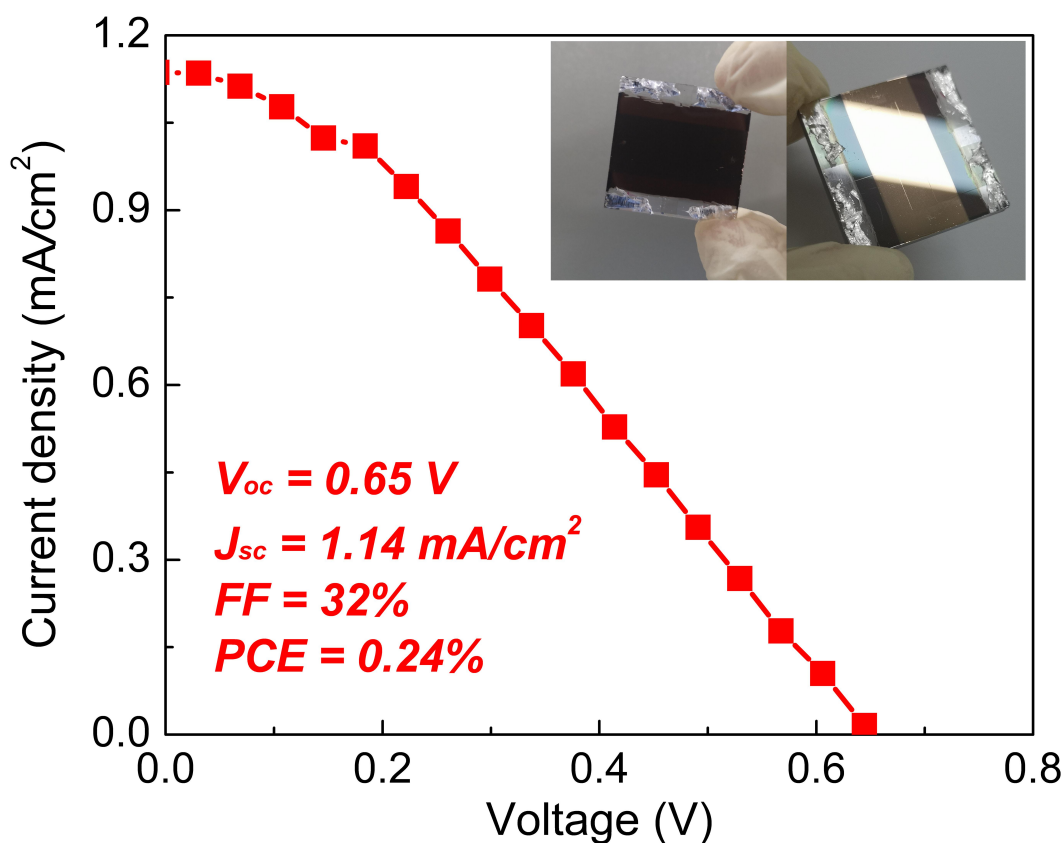


Figure S15. J - V curve of the best performing device with pPDACuBr₄ absorber measured under simulated AM1.5 100 mW/cm² illumination. The inset is digital photos of a pPDACuBr₄-based solar cell.

Table S4. Comparison of initial photovoltaic parameters of devices based on Cu-based organic–inorganic hybrid perovskite materials.

Perovskites	V_{oc} [V]	J_{sc} [mA/cm ²]	FF [%]	PCE [%]	Ref.
(C ₆ H ₅ CH ₂ NH ₃) ₂ CuBr ₄	0.68	0.73	41	0.20	[15]
MA ₂ CuCl ₂ Br ₂	0.26	0.216	32	0.017	[16]
MA ₂ CuCl _{0.5} Br _{3.5}	0.29	0.021	28	0.0017	[16]
pPDACuBr ₄	0.65	1.14	32	0.24	Our work

REFERENCES

- (1) H. Tsai, W. Nie, J. C. Blancon, C. C. Stoumpos, R. Asadpour, B. Harutyunyan, A. J. Neukirch, R. Verduzco, J. J. Crochet, S. Tretiak, L. Pedesseau, J. Even, M. A. Alam, G. Gupta, J. Lou, P. M. Ajayan, M. J. Bedzyk and M. G. Kanatzidis, *Nature*, 2016, **536**, 312–316.
- (2) B. Ding, S. Y. Huang, Q. Q. Chu, Y. Li, C. X. Li, C. J. Li and G. J. Yang. *J. Mater. Chem. A*, 2018, **6**, 10233.

- (3) X. Feng, Y. Dong and D. Jiang, *Cryst Eng Comm*, 2013, **15**, 1508–1511.
- (4) Y. Li, J. Gao, Q. Li, M. Peng, X. Sun, Y. Li, G. Yuan, W. Wen and M. Meyyappan, *J. Mater. Chem.*, 2011, **21**, 6944–6947.
- (5) H. S. Jung and N. G. Park, *Small*, 2015, **11**, 10–25.
- (6) Z. Xiao, W. Meng, J. Wang, D. B. Mitzi and Y. Yan, *Mater. Horiz.*, 2017, **4**, 206–216.
- (7) W. Ke and M. G. Kanatzidis, *Nat. Comm.*, 2019, **10**, 965.
- (8) K. Z. Du, W. Meng, X. Wang, Y. Yan and D. B. Mitzi, *Angew. Chem. Int. Ed.*, 2017, **129**, 1–6.
- (9) Y. Kim, Z. Yang, A. Jain, O. Voznyy, G. H. Kim, M. Liu, L. N. Quan, F. P. Garcia de Arquer, R. Comin, J. Z. Fan and E. H. Sargent, *Angew. Chem. Int. Ed.*, 2016, **55**, 9586–9590.
- (10) X. L. Li, L. L. Gao, B. Ding, Q. Q. Chu, Z. Li and G. J. Yang, *J. Mater. Chem. A*, 2019, **7**, 15722–15730.
- (11) J.-C. Hebig, I. Kühn, J. Flohre and T. Kirchartz, *ACS Energy Lett.*, 2016, **1**, 309–314.
- (12) A. Karmakar, M. S. Dodd, S. Agnihotri, E. Ravera, V. K. Michaelis, *Chem. Mater.*, 2018, **30**, 8280–8290.
- (13) N. Singhal, R. Chakraborty, P. Ghosh, A. Nag, *Chem. Asian*, 2018, **13**, 2085–2092.
- (14) M.-G. Ju, M. Chen, Y. Zhou, H. F. Garces, J. Dai, L. Ma, N. P. Padture and X. C. Zeng, *ACS Energy Lett.*, 2018, **3**, 297–304.
- (15) X. Li, B. Li, J. Chang, B. Ding, S. Zheng, Y. Wu, J. Yang, G. Yang, X. Zhong and J. Wang, *ACS Appl. Energy Mater.*, 2018, **1**, 2709–2716.
- (16) D. Cortecchia, H. A. Dewi, J. Yin, A. Bruno, S. Chen, T. Baikie, P. P. Boix, M. Gratzel, S. Mhaisalkar, C. Soci and N. Mathews, *Inorg. Chem.*, 2016, **55**, 1044–1052.
- (17) P. Yang, G. N. Liu, B. D. Liu, X. D. Liu, Y. B. Lou, J. X. Chen and Y. X. Zhao, *Chem. Commun.*, 2018, **54**, 11638.
- (18) B. Ding, L. Gao, L. Liang, Q. Chu, X. Song, Y. Li, G. Yang, B. Fan, M. Wang, C. Li and C. Li, *ACS Appl. Mater. Interfaces*, 2016, **8**, 20067–20073.
- (19) L.-L. Gao, C.-X. Li, C.-J. Li, G.-J. Yang, *J. Mater. Chem. A*, 2017, **5**, 1548–1557.
- (20) N. J. Jeon, J. H. Noh, Y. C. Kim, W. S. Yang, S. Ryu and S. Il Seol, *Nat. Mater.*, 2014, **13**, 897–903.
- (21) Y. H. Deng, X. P. Zheng, Y. Bai, Q. Wang, J. J. Zhao, J. S. Huang, *Nat. Energy*, 2018, **3**, 560–566.